Radiation Protection Dosimetry (2018), Vol. 180, No. 1–4, pp. 291–295
Advance Access publication 3 February 2018
doi:10.1093/rpd/ncy008

AN ONLINE, RADIATION HARD PROTON ENERGY-RESOLVING SCINTILLATOR STACK FOR LASER-DRIVEN PROTON BUNCHES

Franz Siegfried Englbrecht[1,*], Matthias Würl[1], Francesco Olivari[1], Andrea Ficorella[3,4], Christian Kreuzer[1], Florian H. Lindner[1], Matteo Dalla Palma[3,4], Lucio Pancheri[3,4], Gian-Franco Dalla Betta[3,4], Jörg Schreiber[1,2], Alberto Quaranta[3,4] and Katia Parodi[1]
[1]Department of Medical Physics, Faculty of Physics, Ludwig-Maximilians-Universität München, Garching/München, Germany
[2]Max Planck Institute of Quantum Optics, Garching/München, Germany
[3]Department of Industrial Engineering, University of Trento, Trento, Italy
[4]INFN TIFPA, Trento, Italy

*Corresponding author: franz.englbrecht@physik.uni-muenchen.de

We report on a scintillator-based online detection system for the spectral characterization of polychromatic proton bunches. Using up to nine stacked layers of radiation hard polysiloxane scintillators, coupled to and readout edge-on by a large area pixelated CMOS detector, impinging polychromatic proton bunches were characterized. The energy spectra were reconstructed using calibration data and simulated using Monte-Carlo simulations. Despite the scintillator stack showed some problems like thickness inhomogeneities and unequal layer coupling, the prototype allows to obtain a first estimate of the energy spectrum of proton beams.

INTRODUCTION

Radiotherapy with protons, carbon ions or other particles could be superior to conventional X-ray based radiotherapy, since the dose deposition can be more accurately confined to the tumor region to better spare healthy tissue. Compact laser-ion (LION) accelerators will help to investigate and exploit particle radiotherapy further. LION acceleration exploits the generation of MeV/mm electric field gradients, set up through the interaction of a focused laser pulse with a target, to generate ion bunches. Fields of application are nuclear science, astrophysics and medicine[1, 6, 7]. In medicine, LION bunches will complement studies in particle radiotherapy, as well as in ultra-fast radiobiology and particle radiography.

The scintillator stack presented in this work is designed for diagnostics of polyenergetic proton bunches of up to 20MeV. Bunches can be generated using a 300TW laser system[6, 7]. Such system employs Titanium-sapphire crystals as lasing media (Ti:Sa) to generate 800nm central wavelength light pulses with 4J pulse energy and 30fs pulse duration. These pulses are focused to 2.5mmFWHM on the target (nm – mm thick plastic or metal foils) to achieve an intensity of 10^{20} W/cm^2. Since the LION acceleration mechanism is hence different from conventional radio-frequency based accelerators like cyclotrons, the proton beam characteristics and the demand on the beam diagnostics differ (Tables 1 and 2).

Since the interaction of a laser pulse with the target generates an intense field of electrons, X-rays, protons and other ions inside the experimental vacuum chamber, the wish list of requirements for detectors to be used in LION experiments is challenging.

- Radiation hardness
- Vacuum compatibility
- Selectivity in particle type
- Stand the intense electro-magnetic pulse (EMP)
- Provide an estimate of the proton energy spectrum (not only cut-off)
- Provide online results

Most of the currently employed detectors fail to provide multiple of these features (cp. Table 2).

Upcoming detector systems fulfilling these requirements are time-of-flight detectors using graphite silicon, as well as scintillator-coupled semiconductors[1].

MATERIALS AND METHODS

We manufactured a device for beam energy diagnostics based on scintillators coupled to a pixelated CMOS sensor. This scintillator stack design consists of nine layers of a Teflon support (≈150mm), the radiation hard Polysiloxane scintillator (≈150mm) and a thin layer of aluminized Mylar foil (≈8mm) (cp. Figures 1 and 2). The Teflon serves as support structure in the manufacturing process, since the scintillator is molded warm and liquid onto the structure and the active CMOS detector to enable optical coupling to the CMOS. The direct interconnection of scintillator and the 2 mm SiO_2 layer on

Table 1. Comparison of proton beam characteristics for laser accelerator and medical cyclotron.

	Laser[1, 7]	Cyclotron[2]
Bandwidth	$\Delta E/E \approx 100\%$	$\Delta E/E \approx 0.4\%$
Spectrum	Exponential slope	Monoenergetic
Bunch length	ns	cw/ms
Flux	$10^9 - 10^{10}$ p/ns	$10^9 - 10^{10}$ p/s
Energies	<100 MeV	75 – 250 MeV

Table 2. Listing of the detectors currently used in laser-driven ion acceleration[1].

	Online	Photon sensitive	Energy resol.	Drawbacks
CR-39	—	—	Stacked	Chemistry and microscope
Image plates	—	x	—	Long scanning
Dosimetric film	—	x	Stacked	Long scanning
Magnet and CMOS	x	—	x	Measure B-field, setup sensitive

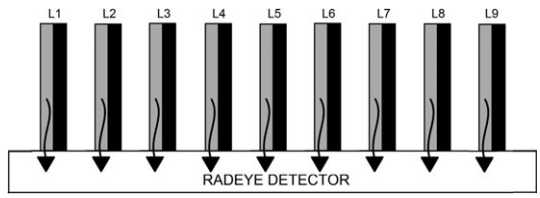

Figure 1. Schematic layout of the design of our radiation hard scintillator stack. The stack consists of nine layers of scintillator (gray), which are readout edge-on by the position sensitive CMOS detector (white). Each Polysiloxane scintillation layer has a thickness of 150mm and is supported by a 150mm Teflon layer (black). Arrows indicate the propagation direction of scintillation photons which enter the CMOS. Crosstalk between layers is suppressed by addition of an aluminized Mylar foil (not shown) between each layer of Teflon and scintillator. Scintillation photons are generated by the proton beam entering the nine layers from the left (beam not shown).

top of the 2mm active Si layer of the CMOS makes optical glue superfluous and reduces potential light losses. The Mylar foil is used to avoid optical crosstalk between layers. Readout is performed using the RadEye CMOS detector (48mm × 48mm pixels). Previous studies showed that this 2.5cm × 5cm sensor, hosting 512 × 1024 pixels, is radiation hard and sensitive to optical photons, protons, electrons and X-rays[8, 9]. To shield the stack from ambient light, laser light and the EMP from the LION acceleration

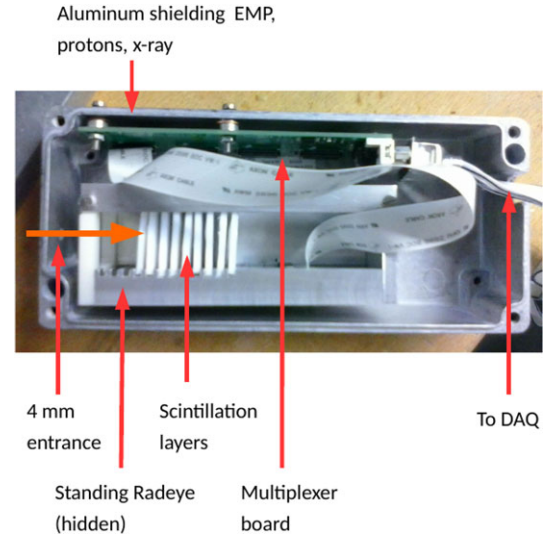

Figure 2. The scintillator stack consisting of an aluminum shielding box, entrance hole for the beam (entering from left), scintillation layers, RadEye detector and readout electronics.

process, the detector is placed in an aluminum housing with a 4mm entrance hole shielded by a 15mm aluminum foil.

Polysiloxane was chosen as scintillating material, since it is liquid during manufacturing, non-toxic, radiation hard and has been shown to have a high light output[4, 5].

A simple estimation of the proton beam high energy cut-off can be done by counting the number of layers showing scintillation signal (Figure 3). We performed calibration measurements by inserting 0–14 layers of glass (each 170mm) into a 22MeV proton beam from a conventional Tandem accelerator and recorded the scintillation distribution (signal S in arbitrary units AU) as a function of glass thickness ($S_{0g} - S_{14g}$, cp. simulations in Figure 3). Two polyenergetic beams were generated by inserting two different passive aluminum plates with different drill-patterns (Figure 4), which modulated the beam in energy and have been manufactured according to dedicated MC simulations (Figures 5 and 7). The scintillation distributions of the two polyenergetic beams (S_{meas}) were decomposed using the measured scintillation distributions for 0–14 glasses. Both signal sets (cp. simulated Figures 3 and 5) were normalized per proton using Faraday-cup measurements. The most distal layer scintillating (e.g. L9 for the simulation in Figure 5) is reconstructed first, using the signal value in the layer $S_{L9,\text{meas}}$. Since scintillation in the most distal layer can be attributed to the highest number of moderators with L9 still scintillating (3 g, cp. Figure 3), the weight $w_{3g} = S_{L9,\text{meas}}/S_{L9,3g}$ can be

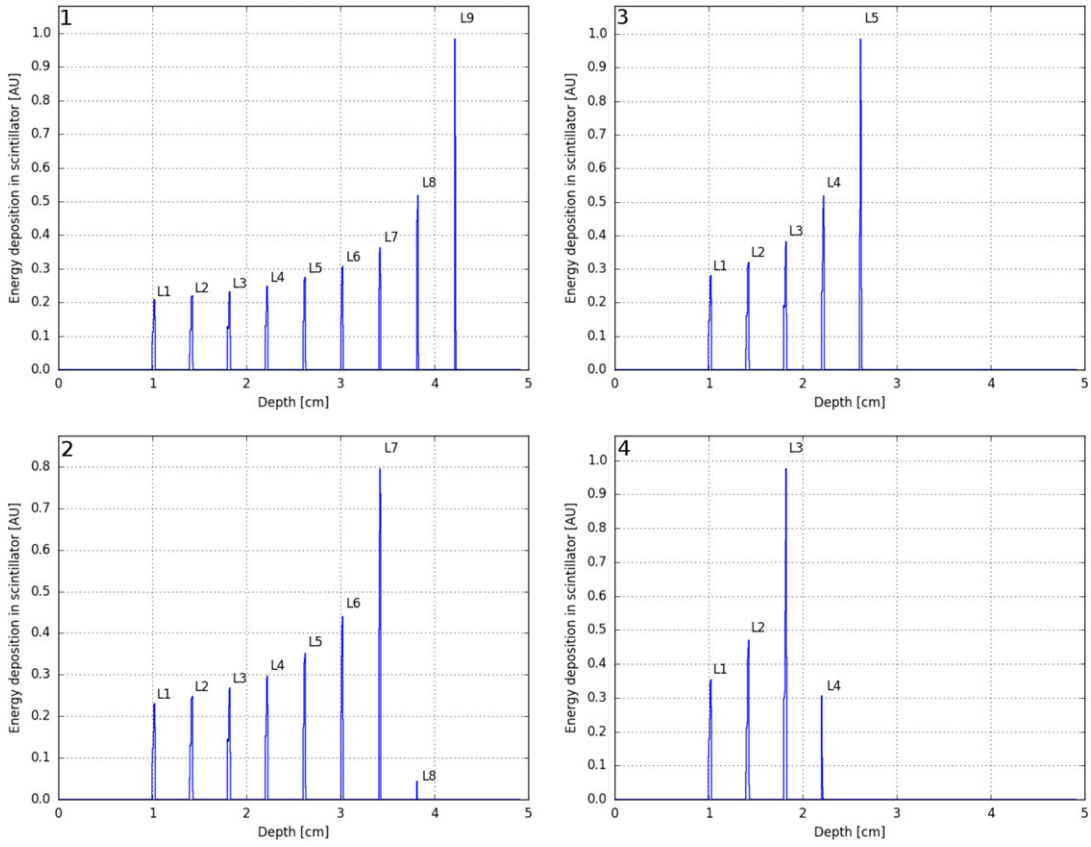

Figure 3. Simulation of monoenergetic proton Bragg peaks in the stack using the FLUKA MC code (compare scheme in Figure 1)[3]. The stack samples nine points of the full depth–dose distribution. Data shows the energy deposition in the scintillation layers for a modulation of 22MeV with 170mm glasses (1: 510mm, 2: 850mm, 3: 1360mm, 4: 1700mm)

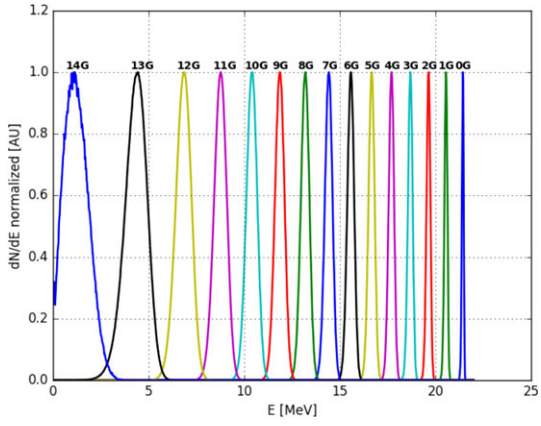

Figure 4. MC simulation of proton energies entering the scintillator stack when modulating a monoenergetic 22MeV proton beam using 0–14 layers of 170mm glass.

calculated. The signal $w_{3g} \cdot S_{3g}$ is then subtracted from the initial S_{meas} and the new signal used to reconstruct the next layer ($S_{L8,\text{meas}}$). The total result is the spectrum $E = \sum_{i=1g}^{14g} w_i \cdot S_i$ (Figure 7).

The stack was placed in a vacuum chamber to avoid beam scattering and energy loss in air, simplify the MC simulations of the experiments and test the stack performance in vacuum (Figure 3). Absolute charge calibration (S/proton) was performed using MC simulations and Faraday-Cup measurements of the impinging beam. The beam current from the accelerator was ranging between 0.8 and 1.3 nA in order to obtain a sufficient scintillation signal level above background.

RESULTS AND DISCUSSION

The results of the calibration measurements using the 170mm glass slices show some deviations from the

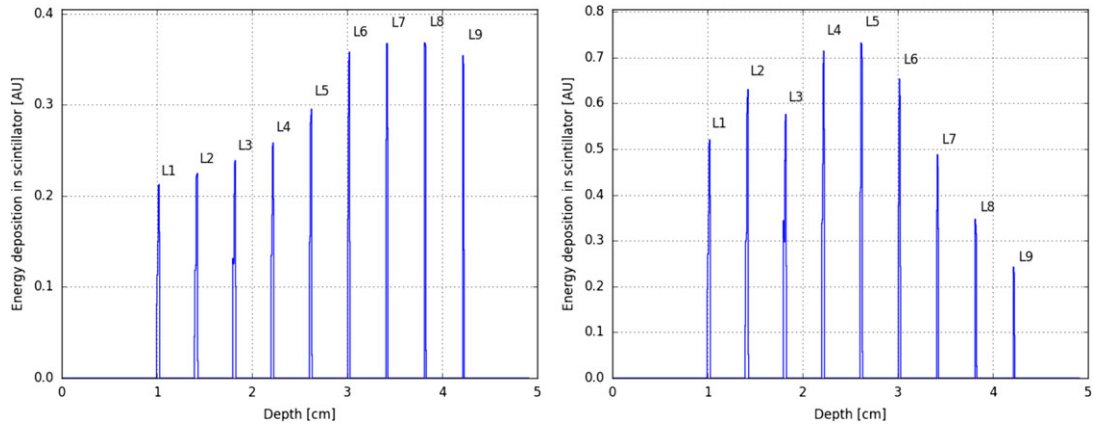

Figure 5. MC simulation of the expected scintillation distributions after inserting the two passive filters. Filter 1 generates to a SOBP (left), Filter 2 an exponential-like proton energy spectrum as from a LION experiment (right).

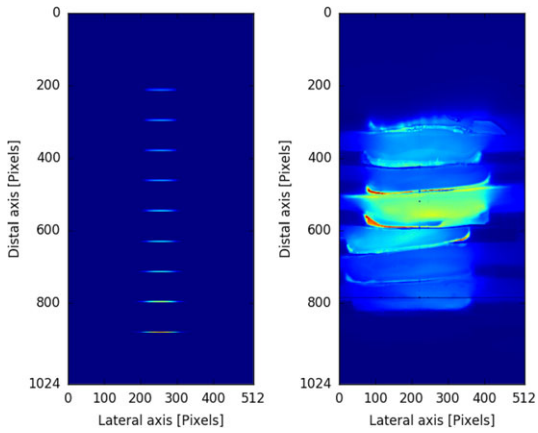

Figure 6. Comparison of expected 2D distribution of scintillation light on the RadEye based on MC simulation (left) and corresponding measurement result (right). Beam enters from the top. The beam energy was degraded using 3 × 170mm glass (compare lineout in Figure 3.1).

idealized MC simulations, which hinder a purely MC-based reconstruction. Most challenging for the reconstruction are several problems: Non-homogeneous response of the layers and laterally along the layers, uncertainties in the thickness of the scintillation and Teflon layers, bright halo-areas in between scintillation layers and non-ideal coupling to the CMOS (Figure 6). Layers six to nine (L6–L9) showed weak response to energy depositions to impinging protons, which is in disagreement with simulation. We attribute the problems to the manual process of the liquid scintillator deposition onto the support structure and a local free flow of the scintillator on the CMOS around the layer positions (cp. Figure 6).

The two expected spectra (From dedicated MC simulations, studying the sensitivity on different beam sizes and hit position of the filter (cp. Figure 7).) are: A spectrum generating a spread out Bragg peak (SOBP) and an exponential-like spectrum (Figure 6) as encountered in LION experiments (Figure 5). The energy resolution using the 14 glass measurements is ≈1.5MeV for $E > 10$MeV and ≈3MeV for $E < 10$MeV (cp. Figures 3, 4 and 7).

CONCLUSION

Our radiation hard scintillator stack prototype allowed us to obtain a first estimate of the proton beam energy, at least by counting the maximum number of scintillating layers. The two passive aluminum filters when inserted into the beam path show, after reconstruction, at least a correlation to the spectrum as obtained by forward MC simulation (Figure 7). Shortcomings were the non-uniform layer coupling, a low scintillation yield and the unknown and non-homogeneous layer thicknesses.

OUTLOOK

Future stack designs for the usage at higher proton energies are under investigation. A 3D-printed support structure will enable a two-sided readout of the scintillator layers and more homogeneous coupling and layer thicknesses. The two-sided readout will allow to judge not only the bunch spectrum, but also the pointing and divergence of the bunch. MC simulations of the improved configuration of 50 scintillation and 50 energy degradation layers will be used to propose a stack layout for the spectral diagnostics of laser-driven proton bunches of up to 100MeV. Such parameters are targeted at our 3PW laser system at

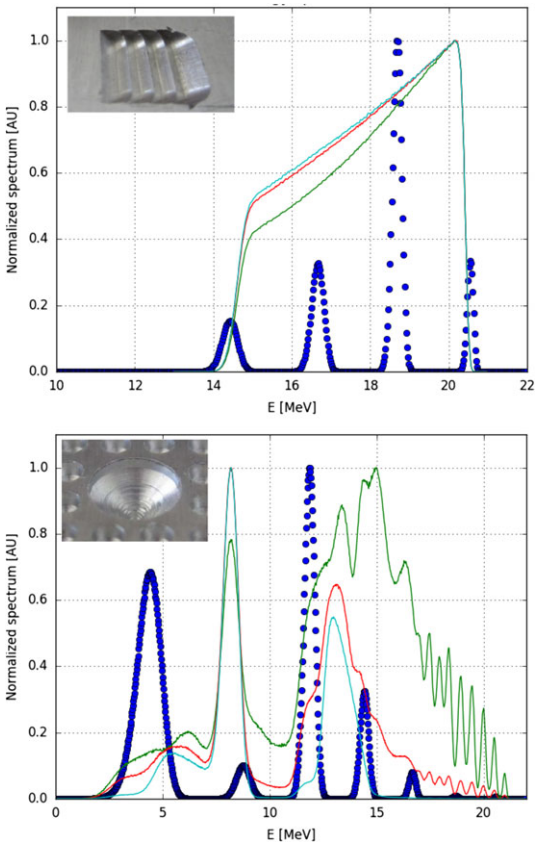

Figure 7. MC simulated proton spectra from two passive filters (top: SOBP-filter, bottom: LION-filter) and spectra reconstructed (blue dots) using calibration data (Figure 4). Inlays show geometrical shape. The three different hit positions of the 22MeV beam give an estimate on the spectra possibly encountered in the experiment (green, red, turquoise), since the filters are hit-position sensitive. The reconstruction is able to give an estimate on the minimum and maximum energy of the spectrum and the spectral shape (Figure 5).

the 'Center for Advanced Laser Applications (CALA)' in Munich, starting in 2018.

ACKNOWLEDGEMENTS

German research foundation (DFG) Cluster of excellence 'Munich Center for Advanced Photonics', International Max Planck Research School IMPRS-APS, Erasmus program of the EU.

REFERENCES

1. Daido, H., Nishiuchi, M. and Pirozhkov, A. S. *Review of laser-driven ion sources and their applications*. Rep. Prog. Phys. **75**, 056401–056472 (2012).
2. Enghardt, W. (2016) *State of the art in particle therapy*. Deutsche Gesellschaft für Medizinische Physik Jahrestagung—Session 'Partikeltherapie I—Novel developments in clinical particle therapy'.
3. Ferrari, A., Sala, P. R., Fasso, A. and Ranft, J. (2005) *FLUKA: a multi-particle transport code*. CERN-2005–10 (2005), INFN/TC_05/11, SLAC-R-773.1
4. Dalla Palma, M., Quaranta, A., Marchi, T., Collazuol, G., Carturan, S., Cinausero, M., Degerlier, M. and Gramegna, F. *Red emitting phenyl-polysiloxane based scintillators for neutron detection*. IEEE Trans. Nucl. Sci. **61-4**, 2052–2058 (2014).
5. Dalla Palma, M., Carturan, S. M., Degerlier, M., Marchi, T., Cinausero, M., Gramegna, F. and Quaranta, A. *Non-toxic liquid scintillators with high light output based on phenyl-substituted siloxanes*. Opt. Mater. **42**, 111–117 (2015).
6. Linz, U. and Alonso, J. *Laser-driven ion accelerators for tumor therapy revisited*. Phys. Rev. Accel. Beams **19**, 124802–124810 (2016).
7. Schreiber, J., Bolton, P. R. and Parodi, K. *Hands-on laser-driven ion acceleration: a primer for laser-driven source development and potential applications*. Rev. Sci. Instrum. **87**, 071101–071110 (2016).
8. Reinhard, S., Draxinger, W., Schreiber, J. and Assmann, W. *A pixel detector system for laser-accelerated ion detection*. JINST **8**, P03008 (2013).
9. Reinhard, S., Granjab, C., Krejcib, F. and Assmann, W. *Test of pixel detectors for laser-driven accelerated particle beams*. JINST **6**, C12030 (2011).